INL/CON-22-70239-Revision-0

Development Of A Photonic Doppler Velocimeter To Verify A Fabry-Perot Velocimeter

May 2023

Changing the World's Energy Future

James A Smith, Bradley C Benefiel, Shaun Pierce Evans

Idaho National Laboratory

INL is a U.S. Department of Energy National Laboratory operated by Battelle Energy Alliance, LLC

INL/CON-22-70239-Revision-0

Development Of A Photonic Doppler Velocimeter To Verify A Fabry-Perot Velocimeter

James A Smith, Bradley C Benefiel, Shaun Pierce Evans

May 2023

Idaho National Laboratory
Idaho Falls, Idaho 83415

http://www.inl.gov

Prepared for the
U.S. Department of Energy
Under DOE Idaho Operations Office
Contract DE-AC07-05ID14517

Development Of A Photonic Doppler Velocimeter To Verify A Fabry-Perot Velocimeter

James A Smith
Measurment Sciences
Idaho National Laboratory
Idaho Falls, USA
James.Smith@INL.gov

Brad C. Benefiel
Experimental Design
Idaho National Laboratory
Idaho Falls, USA
Bradley.Benefiel@inl.gov

Shaun P. Evans
Systems Engineering
Idaho National Laboratories
Idaho Falls, USA
Shaun.Evans@inl.gov

***Abstract*— The laser shock system uses acoustic shockwaves to measure the interface strength of newly designed nuclear fuel plates. The quantitative measurement of interface strength will help understand fuel performance during irradiation. The laser shock technique imparts laser energy into a plate that then creates an acoustic shockwave. The amount of energy in the plate is proportional to the surface velocities measured on the back side of the plate. An accurate determination of surface velocity will enable better fuel performance predictions. The focus of this paper is on the implementation of a Photonic Doppler Velocimeter to corroborate the Fabry-Perot measurements from the laser shock system. Currently, a Fabry-Perot velocimeter takes the velocity measurements that are converted in stress. We have designed and implemented a Photonic Doppler Velocimeter to corroborate the Fabry-Perot measurements, which we discuss here along with implementing the short time fast Fourier transform to demodulate the heterodyne beat frequency into velocities. The Photonic Doppler Velocimeter has successfully corroborated the Fabry-Perot measurements.**

Keywords—photonic Doppler velocimeter, Fabry-Perot cavity, surface velocity, interface strength, bond characterization

I. Introduction

In 2014, the United States (U.S.) National Nuclear Security Administration created the Office of Material Management and Minimization (M^3). M^3 has the responsibility to identify, secure, and remove weapons-usable nuclear materials around the world [1]. M^3 has assumed the U.S. efforts of the former Global Threat Reduction Initiative Convert Program that focused on the conversion of domestic and foreign research reactors from highly enriched uranium to low-enriched uranium (LEU) fuel.

The U.S. High Performance Research Reactor (USHPRR) Fuel Qualification Project is working on the development, qualification, and licensing of novel fuel systems to transition five research reactors and one critical assembly in the U.S. from highly enriched uranium to LEU. The development and selection of the U-10Mo monolithic LEU fuel system are finalized with the emergence and scale up of the chosen fabrication process. The chosen fabrication process involves U-10Mo foils co-rolled with zirconium diffusion barrier interlayers and clad in aluminum alloy 6061 using a hot isostatic pressing process that bonds the two cladding substrates [2].

The laser shock (LS) project is tasked with determining the interface strengths within the fuel plate, which may include cladding-cladding or fuel-cladding interfaces. An overview of the LS technique is shown in Fig. 1 for a sample plate with an interface. A 2.4 Joule laser pulse with a 10 ns pulse width imparts a significant amount of energy into the sample. The resulting shockwave propagates from the front surface to the back surface. A Fabry-Perot (F-P) velocimeter measures the shockwave energy at the backside of the sample, Fig. 1(a) [3–16]. The measured back surface velocity, Fig. 1(b), is used to determine the bulk stress, Fig. 1(c), that propagated through the interface. The resulting bulk stress, σ(t) as shown in Fig. 1(c), is a function of:

- ρ Density
- c Longitudinal speed of sound in the cladding
- u(t) Surface velocity

The interface strength of a bond is determined by the maximum energy that the interface supported prior to debonding. Interface debondings are detected by ultrasonic C-scanning the specimen after each shock laser interrogation. Interrogation usually occurs at the same location to save scarce sample space on fuel plates. Laser energy is increased in steps up to 2.4 Joule or until the interface debonds.

The accurate quantification of interface strength is dependent on the accurate measurement of the back surface velocity reported by the F-P.

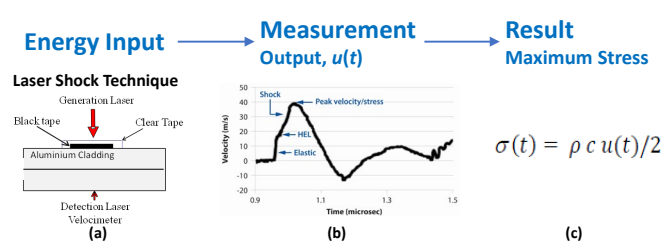

Fig. 1. The LS technique consists of (a) inputting energy into a sample with an interface, (b) measuring the back surface velocity with a velocimeter, and (c) converting the velocity measurement into stress.

Supported by the U.S. Department of Energy, Office of Material Management and Minimization under DOE-NE Idaho Operations Office.

The project needed a method to verify the F-P measurements. Verifying velocity with an independent method ensures quantifiable measurements and confirms the resulting interface strength-stress calculation accuracy. The verification of the LS velocity measurements will allow Idaho National Laboratory's (INL's) results to be traceable and reproduceable with commercial fabricators, external laboratories, and other interface characterization techniques. This paper will focus on the novel development of the Photonic Doppler Velocimeter as an independent measure of shockwave velocity to corroborate F_P measurements.

II. Fabry-Perot Interfeometer

The current LS system uses an F-P etalon to measure surface velocities. The LS F-P velocimeter is well documented in previous research [3–9, 17]. The F-P velocimeter consists of a resonant optical cavity made from two parallel reflecting surfaces (i.e., thin mirrors). Light can pass through the optical cavity only when the light is in resonance within the cavity [17]. The F-P velocimeter is a common choice for in-situ industrial measurements especially since the system uses a large core fiber to transmit and receive laser light. The F-P velocimeter works well on diffuse surfaces, is easy to align, and is effective on most surfaces.

Although the LS F-P velocimeter is an effective measurement tool, the accuracy of the resulting interface strength measurements should be confirmed against measurements of an independent technique. The validated LS interface strength measurements will be used as input to fuel performance models to forecast the integrity of the fuel under different reactor conditions. The LS interface strength measurements will also provide feedback about the fuel plate fabrication process to inform decisions about insertion into a reactor.

The LS system has participated in round robin studies with the original designers and fabricators of the LS system [9] to corroborate the two measurements. Performing round robins are not feasible when we would like to confirm the measurements after LS system modifications and periodic calibration checks. Thus, corroborating the velocimeter is warranted. The development of the corroborating interferometer is the focus of the rest of the paper.

III. Photonic Doppler Velocimeter

This study has chosen the Photonic Doppler Velocimeter (PDV) [18–21] to independently verify the back surface velocity measurements made by the F-P velocimeter. PDV is a heterodyne frequency measurement technique. Heterodyne measurement techniques are established and in common use [18–21]. The fiber-optic implementation of PDV makes the installation and operation of the instrumentation simple, as shown in Fig. 2.

The velocimeter system consists of two lasers and uses single-mode fibers to direct the light. The target laser is injected into Port 1 of an optical fiber circulator. The light exits the circulator via Port 2 into the probe optical fiber. The probe fiber consists of a fiber with a telescoping lens system at the distal end of the fiber that can focus the light onto the target's surface. The back-scattered light is collected by the probe lens system and reinjected into the circulator via Port 2. The reflected light exits

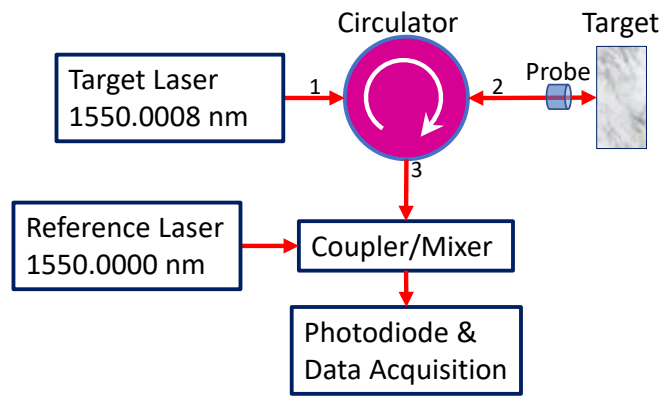

Fig. 2. Schematic diagram of the PDV measurement system.

the circulator via Port 3 and is then mixed with the reference laser in the coupler, which is directed onto a photodiode. The resulting heterodyne signal from the photodiode is digitized and processed to provide surface velocity with time.

The PDV system is a heterodyne system because the two lasers are operating at slightly different wavelengths. The two frequencies are tunable around 1,550 nm. The target laser is nominally set at 1,550.008 nm, and the reference laser is nominally set at 1,550.000 nm. The mixing of the laser light between the two lasers produces a beat frequency nominally at 650 MHz. Doppler shifts in the target light are caused by surface motion of the target and modulates the beat frequency.

The Doppler shift is a function of the measured beat frequency and the frequency difference between the target and reference laser, as shown in (1):

$$f_d = B - (f_T - f_R) \tag{1}$$

where,

- f_d is the Doppler shift
- B is the measured beat signal
- f_T is the optical frequency of target laser
- f_R is the optical frequency of the reference laser

The surface velocity is determined by the Doppler shift and wavelength of the target laser as given by (2):

$$v = \left(\frac{\lambda_T}{2}\right) f_d \tag{2}$$

where,

- v is the surface velocity
- λ_T is the wavelength of the target laser
- f_d is the Doppler shift caused by surface motion

Processing the photodiode signal yields the Doppler shift, f_d. As shown in Fig. 2, a digital sampling oscilloscope digitizes the

photodiode signal. Digitized heterodyne beat frequency processing to obtain f_d is discussed in the next section.

IV. Heterodyne Signal Processing

The heterodyne beat frequency is frequency modulated by the motion of the targets surface. The modulation and demodulation of the heterodyne carrier frequency is equivalent to principles used in frequency modulated (FM) radios. The surface motion is encoded by inducing frequency shifts, via the Doppler effect, into the heterodyne carrier frequency. The FM carrier is then demodulated to reproduce f_d with time.

For the PDV system, the demodulation scheme used is the short time fast Fourier transform (STFFT) [22–27]. The STFFT is a Fourier-transform-based technique used to define the sinusoidal frequency, amplitude, and phase content of small time-segments within a signal as the signal evolves over a longer time span. The process to compute the STFFT is to section an extended time signal into smaller time segments of equal length. The standard Fast Fourier Transform (FFT) is computed separately on each smaller time segment. The FFT results for each time segment are then arranged in chronological order and displayed. Plotting varying spectra with time is known as a spectrogram, a specific type of waterfall plot.

A simulation verified the STFFT demodulation technique is appropriate for corroborating velocity measurements from the F-P. A damped sine wave with a frequency of 3 MHz and a displacement amplitude of 12.34 µm was used in the simulation. The resulting maximum velocity is approximately 205 m/s. Fig. 3 shows the simulated surface displacements that will Doppler shift the simulated target probe beam. A first arrival and two reflections are simulated.

The heterodyne carrier frequency, 850 MHz, is then phase modulated, generating B, by the simulated surface displacements. The phase modulation of the carrier frequency is naturally converted into Doppler shifted frequency variations, f_d. The STFFT spectrogram, Fig. 4, shows the spectrogram and resulting Doppler shifts encoded onto the heterodyne beat frequency.

The arrival time for the Doppler shifted signals resulting from the first arrival and reflections match. Although the surface has been displaced in terms of distance, the Doppler shift converts the time varying displacements into frequency shifts proportional to surface velocities or equivalent to the derivative of the displacements. Thus, the shape of the displayed wave form is different from the source displacement motion.

The Doppler shift as a function of time is obtained by finding the maximum amplitude spectral component at each point in time in the spectrogram. Once the frequencies with the maximum amplitudes are selected from the beat signal, B, a quiescent region within the spectrogram is used to determine the heterodyne beat frequency, $(f_T - f_R)$. The Doppler shift, f_d, with time is then found by using (1). The surface velocity can then be calculated by (2).

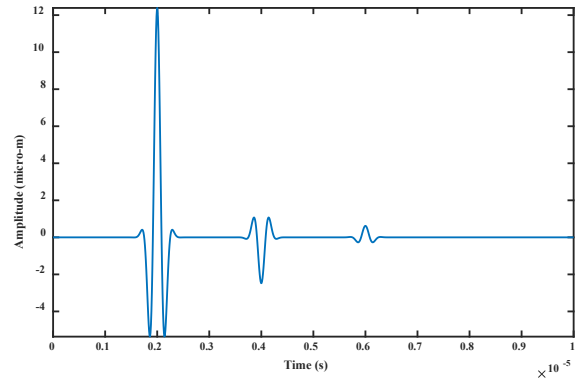

Fig. 3. A simulated damped sine wave with a frequency of 3 MHz and a displacement amplitude of 12.34 µm is used to Doppler shift the simulated target probe beam.

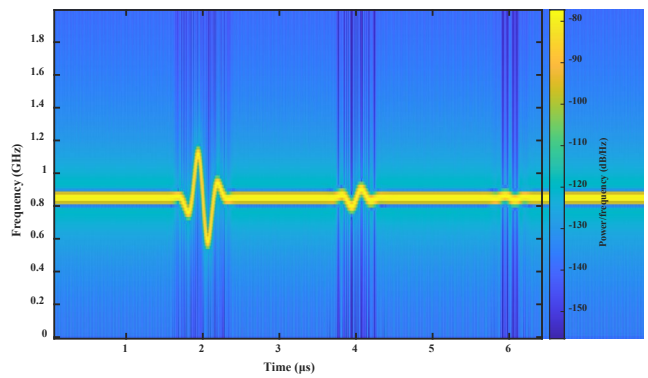

Fig. 4. STFFT spectrogram showing the Doppler shifts resulting from the simulated displacements.

Fig. 5 shows the comparison between the measured and original input velocities. The input velocity has been calculated by taking the first derivative of the input displacements. The two line graphs are in reasonable agreement. There are some differences noted especially at lower velocities. The digital quantization error in the measured signal can be seen in the graph. The quantization error in the measured data is 15.14 m/s for measurement settings:

- Sample rate 20 G Sa/s
- Points within the FFT time window 1,024
- Target wavelength 1,150 nm

Unfortunately, reducing the quantization error by increasing the FFT time window is counterproductive. The longer time window blurs and reduces the effects from dynamic changes. For these data, 1,024 points is the optimum compromise between velocity accuracy and dynamic bandwidth. For the purposes of this work, the quantization error of 15.14 m/s is small enough to corroborate the measurements made by the F-P. The goal is to confirm that the F-P measurements are reasonable and not to calibrate the F-P system. If a finer resolution is needed in the future, the heterodyne processing techniques described in

[28] can be used to obtain a better PDV resolution, as well as other standard heterodyne demodulation methods.

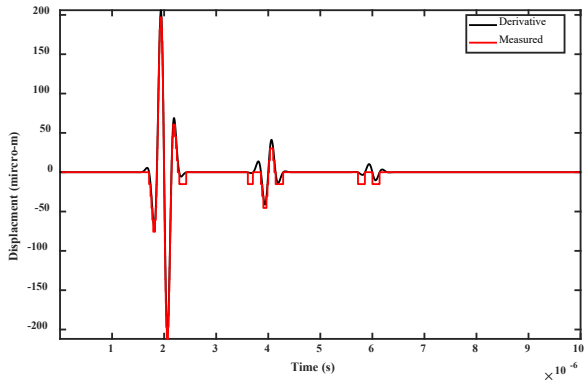

Fig. 5. Comparison between the measured and input velocities resulting from the simulated surface displacements is shown.

V. Experiment And Discussion

The basic experimental setup is shown in Fig. 1(a) and discussed in detail in [3–9]. As shown in Fig 1(a), a high-energy laser pulse (up to 2.4 J) generates a shock wave that propagates through the test sample. The interferometers measure the surface velocity on the backside. From the backside velocity measurements, the amount of stress making it to the back surface can be calculated as outlined in Fig. 1.

The velocimeters monitor the back surface motion by focusing light from a target laser onto the plates surface. Since both the PDV and F-P velocimeter are fiber based, the probe heads can be switched in and out in an expedient manner. The fixtures holding the probe heads are designed so both probes only require minor re-alignments when swapped. Care is taken to ensure that velocimeter interrogation locations are accurately aligned with the epicenter of the generation laser. Fig. 1(b) shows the structure of the first arrival as measured by the F-P velocimeter.

The initial tests consisted of interrogating an Al 6061 T6 plate that is 25.4 × 100 × 1.3 mm with an as-machined surface. The shock laser energy for both the PDV and F-P measurements was 2.4 J. Identical containment layers were used to increase the efficiency of the conversion of laser energy to the acoustic shock wave. Two interrogation locations were used on the same plate.

The measurements from the PDV will be discussed first. The resulting PDV spectrogram from the laser-generated shock wave is shown in Fig. 6. The spectrogram shows the modulation of the beat frequency (yellow trace) at a nominal frequency of 650 MHz. Note that there are multiple harmonics and a sub-harmonic present with the beat frequency due to distortion in the generation of the heterodyne signal. Only the beat frequency will be discussed because all the harmonics contain the same velocity information. The first arrival can be seen near 1.8 µs. Multiple reflections are spaced out throughout the time series. The information contained in the spectrogram can be converted to velocity measurements.

The resulting velocity plot is shown in Fig. 7. The velocity trace shows definite signatures, but the quantization noise makes the graph look discontinuous and hard to interpret. The quantization noise is a consequence of using the FFT to demodulate the signal. The first arrival of the shock wave is

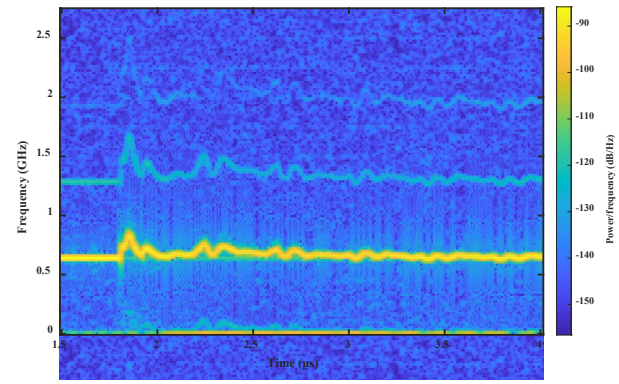

Fig. 6. Spectrogram generated from the PDV that shows the Doppler shifts caused by the arrival on the back face of the plate from a shock wave.

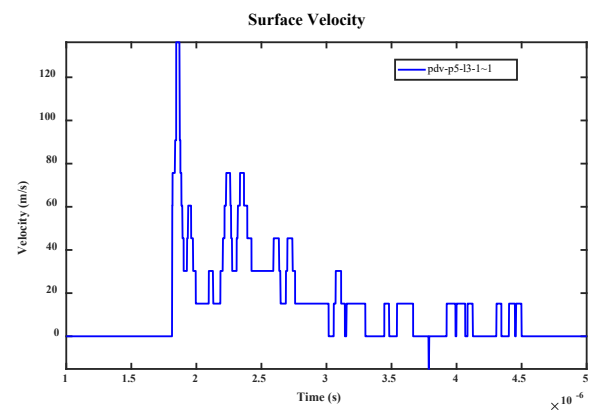

Fig. 7. The fully demodulated PDV signal expressed as surface velocity. The trace clearly shows the arrival of the first acoustic wave and the sharp steps caused by quantization error.

clearly seen, but the reflections have low contrast and are hard to identify. The presentation in the spectrogram confirms the peaks in the demodulated PDV signal as the arrival of acoustic energy.

The comparison of the F-P measurements with the PDV measurements is shown in Fig. 8. The two velocimeters show excellent agreement. With the F-P plotted with the PDV, the F-P trace confirms that the peaks in the PDV trace are acoustic arrivals. The timing and locations of the structures within the acoustic wave are present and match between the two velocimeter signals.

This validating experiment clearly shows that the PDV system corroborates the velocity measurements made by the LS interface characterization system.

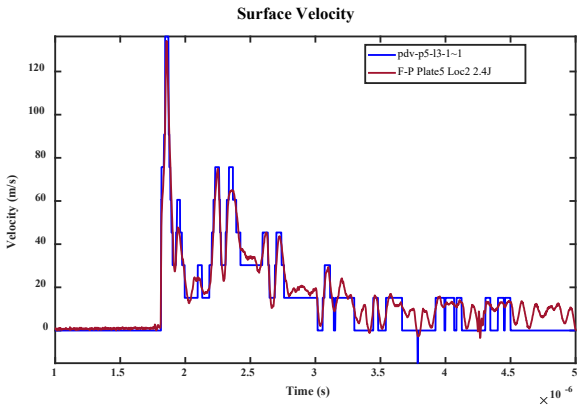

Fig. 8. The comparison of the F-P measurements with the PDV measurements show that the two velocimeters are within the digitization error of the PDV for timing and amplitude.

VI. Conclusion

The LS technique is being developed to measure the interface strength of interfaces in nuclear plate fuel, which may be cladding-cladding or fuel-cladding interfaces. The interface strength of an interface is determined by measuring the maximum velocity that the interface supported prior to debonding. The measured maximum velocity at the back surface can be converted into stress that can be used to help understand fuel performance under irradiation. Thus, the accurate measurement of surface velocity is salient.

A verification system has been developed based on the PDV. The high-level configuration of the PDV was discussed. The STFFT was chosen to demodulate the beat frequencies and convert frequency shifts into velocities. The heterodyne demodulation processing was verified using simulated surface displacements. When the PDV was verified, it was used to corroborate the F-P measurements.

The F-P velocimeter was corroborated by the PDV. Initial testing has shown that the velocity traces resulting from an acoustic wave are in excellent agreement. Velocity measurement verification with an independent technique validates quantifiable measurements and enables proven estimates from interface strength-stress calculations. Verified velocity measurements allow INL's results to be traceable and reproduceable with commercial fabricators, external laboratories, and other interface strength techniques. The PDV system is simple enough to perform verification checks on a regular basis.

Acknowledgment

The authors would like to thank the USHPRR Fuel Qualification Project, and Battel Energy Alliance for providing support and infrastructure. Thank you to the INL Research Center machine shop for machining the aluminum test plates and the INL editorial staff for their excellent reviews. This manuscript has been authored by Battelle Energy Alliance, LLC under Contract No. DE-AC07-05ID14517 with the U.S. Department of Energy. The United States Government retains and the publisher, by accepting the article for publication, acknowledges that the U.S. Government retains a nonexclusive, paid-up, irrevocable, world-wide license to publish or reproduce the published form of this manuscript, or allow others to do so, for U.S. Government purposes.

References

[1] U.S. Department of Energy. "Global Threat Reduction Initiative (GTRI): PNNL GTRI Convert Program Program Management Plan." [Online]. https://www.pnnl.gov/main/publications/external/technical_reports/PNNL-22443.pdf. accessed November, 2022.

[2] M. A. Marshall, I. Glagolenko, D. O. Choe, and J. W. Nielsen. "Mini-plate irradiation testing in ATR to support U-Mo fuel qualification for high performance research reactor conversion." *T. Am. Nucl. Soc.*, Orlando, FL, USA, vol. 119, no. 1, pp. 419–422, Nov. 2018. https://www.ans.org/pubs/transactions/article-44252/.

[3] J. A. Smith, B. C. Benefiel, and C. L. Scott. "Remote fiber based velocimeter for interface strength measurements." *2021 IEEE I2MTC, IEEE IMS*, Virtual Conference, May 17–20, 2021. https://doi.org/10.1109/ I2MTC50364.2021.9459939.

[4] J. A. Smith, M. Choquet, and D. Lévesque. "Design of a laser shock system for a remote nuclear radiation environment." *AIP Conf. Proc.*, vol. 2102, pp. 060002, 2019. https://doi.org/10.1063/1.5099792.

[5] J. A. Smith, C. L. Scott, B. C. Benefiel, and B. H. Rabin. "Interface characterization within a nuclear fuel plate." *Appl. Sci.*vol. 9, no. 2, pp. 249, 2019. https://doi.org/10.3390/app9020249.

[6] M. Perton, D. Lévesque, J. -P. Monchalin, M. Lord, J. A. Smith, and B. H. Rabin. "Laser shockwave technique for characterization of nuclear fuel plate interfaces." *AIP Conf. Proc.*, vol. 1511, pp. 345, 2013. https://doi.org/10.1063/1.4789068.

[7] J. M. Lacy, J. A. Smith, and B. H. Rabin. "Developing a laser shockwave model for characterizing diffusion bonded interfaces." *AIP Conf. Proc.*, vol. 1650, pp. 1376, 2015. https://doi.org/10.1063/1.4914752.

[8] J. A. Smith, J. M. Lacy, D. Lévesque, and J.-P. Monchalin. "Use of the hugoniot elastic limit in laser shockwave experiments to relate velocity measurements." *AIP Conf. Proc.*, vol. 1706, pp. 080005, 2016. https://doi.org/10.1063/1.4940537.

[9] J. A. Smith, et al. "Further investigation of surface velocity measurements for material characterization in laser shockwave experiments." *AIP Conf. Proc.*, vol. 1949, pp. 180001, 2018. https://doi.org/10.1063/1.5031630.

[10] J. L. Vossen. "Measurements of film–substrate bond strength by laser spallation." ASTM Spec. Tech. Publ. Am. Soc. Test. Mater., vol. 640, pp. 122–133. https://doi.org/10.1520/STP38629S.

[11] V. Gupta, et al. "Measurement of interface strength by laser-pulse-induced spallation." *Mater. Sci. Eng. A*, vol. 126, no. 1–2, pp. 105–117, 1990. https://doi.org/10.1016/0921-5093(90)90116-K.

[12] J. Yuan, V. Gupta, and A. Pronin. "Measurement of interface strength by the modified laser spallation technique: I. Experiment and simulation of the spallation process." *J. Appl. Phys.*, vol 74, no. 4, pp. 2388–2397, 1993. https://doi.org/10.1063/1.354700.

[13] J. Yuan, V. Gupta, and A. Pronin. "Measurement of interface strength by the modified laser spallation technique: III. Experimental optimization of the stress pulse." *J. Appl. Phys.*, vol. 74, no. 4, pp. 2405–5107, 1993. https://doi.org/10.1063/1.354700.

[14] C. Bolis, et al. 2007. "Physical approach to adhesion testing using laser-driven shock waves." *J. Phys. D: Appl. Phys.*, vol. 40, no. 10, pp. 3155–3163, 2007. https://doi.org/10.1088/0022-3727/40/10/019.

[15] M. Arrigoni, et al. 2006. "Comparative study of three adhesion tests (EN 582, similar to ASTM C633, LASAT (LASer Adhesion Test), and bulge and blister test) performed on plasma sprayed copper deposited on aluminum 2017 substrates." *J. Adhes. Sci. Technol.*, Vol. 20, no. 5, pp. 471–487, 2006. https://doi.org/10.1163/156856106777144336.

[16] V. Gupta and J. Yuan. "Measurement of interface strength by the modified laser spallation technique. II. Applications to metal/ceramic interfaces." *J. Appl. Phys.*, vol. 74, no. 4, pp. 2397–2404, 1993. https://doi.org/10.1063/1.354699.

[17] M. Arrigoni, et al. "Laser doppler interferometer based on a solid Fabry-Perot etalon for measurement of surface velocity in shock

experiments" *Meas. Sci. Technol*., vol. 20, no.1, pp. 015302, 2009. https://doi.org/10.1088/0957-0233/20/1/015302.

[18] D. B. Holtkamp. "Survey of optical velocimetry experiments - applications of PDV, a heterodyne velocimeter." *2006 IEEE MG-XVI*, pp. 119–128, 2006. https://doi.org/10.1109/MEGAGUSS.2006.4530668.

[19] O. T. Strand, D. R. Goosman, C. Martinez, and T. L. Whitworth. "Compact system for high-speed velocimetry using heterodyne techniques." *Rev. Sci. Instrum.*, vol. 77, no. 8, pp. 083108, 2006. https://doi.org/10.1063/1.2336749.

[20] D. H. Dolana. "Extreme measurements with photonic Doppler velocimetry (PDV)." editors-pick, *Rev. Sci. Instrum*., vol. 91, no. 5, pp. 051501, 2020. https://doi.org/10.1063/5.0004363.

[21] "Photonic Doppler Velocimetry application note," Quantifi Photonics, [Online]. QP_AppNote_PDV_v1.1.pdf (quantifiphotonics.com), accessed 11/20/2022.

[22] V. Agarwal, J. A. Smith, and V. C. Kirkpatrick. 2021. "Predictive data analytics framework using advanced test reactor acoustic data." INL/EXT-21-64432, Idaho National Laboratory. https://www.osti.gov/biblio/1897716.

[23] E. Sejdić, I. Djurović, and J. Jiang. "Time-frequency feature representation using energy concentration: An overview of recent advances." *Digit. Signal Process*., vol. 19, no. 1, pp. 153–183, 2009. https://doi.org/10.1016/j.dsp.2007.12.004.

[24] E. Jacobsen and R. Lyons. "The sliding DFT." *IEEE Signal Process. Mag*., vol. 20, issue 2, pp. 74–80, 2003. https://doi.org/10.1109/MSP.2003.1184347.

[25] J. B. Allen. "Short time spectral analysis, synthesis, and modification by discrete Fourier transform." *IEEE Trans. Acoust., Speech, Signal Process*., vol. 25, no. 3, pp. 235–238, 1977. https://doi.org/10.1109/TASSP.1977.1162950.

[26] J. O. Smith III. 2011. "Overlap-add STFT processing: in Spectral Audio Signal Processing." 2nd ed., *W3K Publishing*, 2011. http://books.w3k.org.

[27] "Help center: stft." *MathWorks*, https://www.mathworks.com/help/releases/R2021a/signal/ref/stft.html?s_tid=doc_ta. accessed November 11, 2022.

[28] J. A. Smith and C. P. Burger. "Digital phase demodulation in heterodyne sensors." *Opt. Eng*., vol. 34, no. 9, pp. 2793–2801, 1995. https://doi.org/10.1117/12.212980.